

PCCP

Accepted Manuscript



This is an *Accepted Manuscript*, which has been through the Royal Society of Chemistry peer review process and has been accepted for publication.

Accepted Manuscripts are published online shortly after acceptance, before technical editing, formatting and proof reading. Using this free service, authors can make their results available to the community, in citable form, before we publish the edited article. We will replace this *Accepted Manuscript* with the edited and formatted *Advance Article* as soon as it is available.

You can find more information about *Accepted Manuscripts* in the [Information for Authors](#).

Please note that technical editing may introduce minor changes to the text and/or graphics, which may alter content. The journal's standard [Terms & Conditions](#) and the [Ethical guidelines](#) still apply. In no event shall the Royal Society of Chemistry be held responsible for any errors or omissions in this *Accepted Manuscript* or any consequences arising from the use of any information it contains.

1 **Dissipative Particle Dynamics Simulation Study of**
2 **Poly(2-Oxazoline)-based Multicompartment Micelle Nanoreactor**

3
4
5 Byeong Jae Chun,^{1,2} Christina Clare Fisher² and Seung Soon Jang^{2,3,4*}
6
7
8

9 ¹ School of Chemical & Biomolecular Engineering, Georgia Institute of Technology, 311
10 Ferst Drive NW, Atlanta, Georgia 30332-0100, USA

11 ² Computational NanoBio Technology Laboratory, School of Materials Science and
12 Engineering, Georgia Institute of Technology, 771 Ferst Drive NW, Atlanta, Georgia
13 30332-0245, USA

14 ³ Institute for Electronics and Nanotechnology, Georgia Institute of Technology, Atlanta, GA,
15 USA

16 ⁴ Parker H. Petit Institute for Bioengineering and Bioscience, Georgia Institute of Technology,
17 Atlanta, GA, USA
18
19

* To whom correspondence should be addressed.
Professor Seung Soon Jang, E-mail: SeungSoon.Jang@mse.gatech.edu

20 **ABSTRACT**

21 We investigate multicompartment micelle consisting of poly(2-oxazoline)-based
22 triblock copolymers for nanoreactor application, using DPD simulation method to
23 characterize the internal structure of micelle and the distribution of reactant. The DPD
24 simulation parameters are determined from the Flory-Huggins interaction parameter (χ_{FH}).
25 From the snapshots of the micellar structures and radial distribution function of polymer
26 blocks, it is clearly presented that the micelle has the feature of the multicompartment. In
27 addition, by implementing the DPD simulations in the presence of reactants, it is found that
28 Reac-C4 and Reac-OPh are well associated with the hydrophilic shell of the micelle whereas
29 other two reactants such as Reac-Ph and Reac-Cl are not incorporated into the micelle. From
30 our DPD simulations, we confirm that the miscibility (solubility) of reactant with the micelle
31 has strong correlation with the rate of hydrolysis kinetic resolution. Utilizing accurate
32 methods evaluating accurate χ_{FH} parameters for molecular interactions in micelle system, this
33 DPD simulation can have a great potential to predict the micelle structures consisting of
34 designed multiblock copolymers for useful reactions.

35
36
37
38
39
40
41
42
43
44

Keywords: hydrolytic kinetic resolution, multicompartment micelle, dissipative particle
dynamics simulation, Flory-Huggins interaction parameter

45 **1. INTRODUCTION**

46 Multicompartment micelle has gained intensive attention in recent catalysis chemistry
47 community.¹⁻⁸ This material contains multiple well-defined spaces in nanoscale structure,
48 which has shown great potentials for nanoreactor technology.¹⁻¹⁰ Owing to the successful
49 progress in fine synthesis in polymer chemistry, well-defined architecture in multi-block
50 copolymer chain leads to a highly controlled morphologies and functionalities of their
51 aggregates.⁶ Especially, the placement of reactive substrates or catalysts on the hydrophobic
52 blocks results in highly localized compartmental space in the micellar core in aqueous solvent
53 environment.^{4, 6, 9-11} Besides, the hydrophilic shell of micelle can protect these sites from any
54 undesirable environments such as solvents and impurities which can cause deactivation of
55 chemical reaction or degradation of products.^{2, 4, 7, 8, 11, 12}

56 According to the report from O'Reilly and coworkers,^{3, 5, 13} smart micelle
57 nanoreactor with a selectivity towards reactants can be generated through introducing specific
58 interactions such as hydrogen bonding, ionic and hydrophobic interactions, implying that
59 reactive catalysts can be embedded in such nanoreactors. Since catalysts are highly
60 localized and encapsulated within the core of micelle, the accessibility of reactants to the
61 reactive core is one of the most crucial factors in developing successful micelle-based
62 nanoreactors. For instance, Weck and coworkers^{4, 11} have studied the poly(2-oxazoline)s
63 (POXs) based shell cross-linked multicompartment (SCM) micelle which can be utilized as
64 nanoreactor for the hydrolysis kinetic resolution (HKR) of epoxides. Although the
65 recyclability of catalysts was enhanced by cross-linking the shells in the micelle, it was
66 observed that the HKR of some epoxides was carried out in the SCM micelle nanoreactor
67 with unexpectedly slow rate: the HKR of epichlorohydrin with Co(III)-salen (catalyst) was
68 completed within 5 hours without using micelle, whereas it was not completed in the micelle

69 even after 24 hours. This result might be due to the shell of micelle blocking the reactive sites
70 as a structural barrier in the micelle. In this case, the transport or permeation of reactant
71 through such structural barrier plays an important role for determining the rate of the HKR of
72 epoxides.

73 In our previous study,¹⁴ regarding the structural barrier as a permeation barrier, we
74 investigated the correlation of Flory-Huggins parameter (χ) with the reaction rate of HKR
75 using full-atomistic molecular dynamics (MD) simulation method. The Flory-Huggins
76 parameter (χ) is a measure of the solubility (or miscibility) of reactants with the micelle,
77 which is a main governing factor for the permeability of the reactants. Although our full-
78 atomistic MD simulations successfully described the association of reactants and products
79 with the micelle as observed in experiment,¹⁴ it was not possible to characterize the
80 distribution of reactants throughout the entire multicompartment micelle with large
81 dimension using such full-atomistic MD simulation. Thus, the details of the reactant
82 distribution in each compartment and at the interface between the compartments remains
83 veiled up to date.

84 In this study, we investigated the structure of micelle consisting of POX-based
85 triblock copolymers and its association with the reactants using dissipative particle dynamics
86 (DPD) simulation method. DPD simulation method developed by Hoogerbrugge and
87 Koelman^{15, 16} has been successfully employed to study the microstructure and properties of
88 polymer phases,^{17, 18} the hydrodynamic behavior of complex fluids,^{16, 19-22} the microphase
89 separation of polymer mixtures.²³⁻²⁶ Especially it is noted that the self-assembled structures of
90 multicompartment micelles has been intensively characterized using DPD simulation
91 method.²⁷⁻³² Inspired by these efforts, we implemented the DPD simulations to elucidate the
92 structure of micelle as a self-assembly of triblock copolymers and the distribution of reactant

93 molecules within the micelle.

94

95 **2. MODELS AND SIMULATION METHODS**

96 **2.1. Models**

97 In the scheme of DPD simulation, the atomistic details of polymer structure are
98 replaced by simplified bead-spring model, so-called coarse-grained model, whose individual
99 beads corresponds to a group of atoms.^{15, 16, 19} In this study, three POX derivatives were
100 expressed using few number of particles as shown in Figure 1. This coarse-graining was
101 carried out using molecular surface area of monomeric units which was evaluated from the
102 solvation free energy as reported in our previous paper.¹⁴ The ratio of surface area is almost
103 PSCoX:PBOX:PMOX = 1:4:8. Then, we ran MD simulations for equilibrium conformations and
104 found that PSCoX has more compact molecular structure. Thus, we decided to use 1:3:6 ratio,
105 meaning that the numbers of monomers to have similar surface area are 6, 2, and 1 for PMOX,
106 PBOX, and PSCoX, respectively. Similarly, the reactant and product molecules were also
107 coarse-grained as presented in Table 1. Although the yellow block B has the reactive triple
108 bond at the end of the side chain for the formation of cross-linked micelle, we simulated
109 micelle without cross-linking in this study. However, we left the block B to keep its
110 molecular interaction with reactants.

111 Here, we need to emphasize the nature of coarse-grained model for DPD simulation
112 employed in this study: in addition to the structural coarse-graining by lumping atoms into
113 large beads, the interactions between coarse-grained beads are described by Flory-Huggins χ
114 parameters which implicitly reflect all the detailed atomistic interactions such as van der
115 Waals, electrostatic and hydrogen bond interactions. Although the model loses most of the
116 atomistic details via this aggressive simplification, the phase separation or segregation can be

117 efficiently simulated using DPD simulation compared to traditional MD simulation.

118

119 2.2. DPD Simulation Details

120 The momenta and position vectors of the DPD particles are governed by Newton's
121 equations of motion:^{15, 16, 19}

$$122 \quad \frac{d\vec{r}_i}{dt} = \vec{v}_i, \quad m_i \frac{d\vec{v}_i}{dt} = \vec{f}_i \quad (1)$$

123 where \vec{r}_i, \vec{v}_i and m_i are the position, velocity, and mass of the i -th particle, respectively. The
124 force \vec{f}_i acting on each particle in the DPD simulation consists of three parts as shown by
125 the following equation:

$$126 \quad \vec{f}_i = \sum_{j \neq i} (F_{ij}^C + F_{ij}^D + F_{ij}^R) \quad (2)$$

127 where F_{ij}^C, F_{ij}^D , and F_{ij}^R are denoted for the conservative force, the dissipative force, and the
128 random force. The three forces are considered within a certain cutoff radius r_c . The
129 conservative force is a soft repulsion acting along the line of centers and is given by

$$130 \quad F_{ij}^C = \begin{cases} a_{ij}(1 - r_{ij}/r_c)\hat{r}_{ij} & (r_{ij} < r_c) \\ 0 & (r_{ij} \geq r_c) \end{cases} \quad (3)$$

131 where a_{ij} and r_{ij} denote a maximum repulsion force and distance between particles i and j ,
132 respectively, and \hat{r}_{ij} denotes a unit vector directing from particle i to particle j . The
133 parameters for repulsion between particles of different types are obtained as a function of the
134 Flory-Huggins interaction parameter χ_{ij} calculated from the Hildebrand solubility parameter
135 (δ). The repulsive parameter (a_{ij}) is expressed as follows:¹⁹

$$136 \quad a_{ij} = a_{ii} + 3.27\chi_{ij} \quad (4)$$

137 According to the regular solution theory, χ_{ij} can be calculated from Hildebrand solubility
 138 parameters:

$$139 \quad \chi_{ij} = \frac{V_m(\delta_i - \delta_j)^2}{RT} \quad (5)$$

140 where δ_i , V_m , R and T are the Hildebrand solubility parameter of particle i , the mixed
 141 molar volume of particles, gas constant, and temperature (300 K). In order to evaluate the
 142 Hildebrand solubility parameters (δ_i), we prepared three pure systems for PMOX (DP=100,
 143 2 chains), PBOX (DP=100, 2 chains) and PSCoX (DP=30, 2 chains) and ran NPT MD
 144 simulations for 5 ns in equilibrium state. From such equilibrium MD simulations, δ_i was
 145 calculated by $\delta = [(\Delta H_v - RT)/V_m]^{1/2}$ where ΔH_v is the heat of vaporization, and V_m is the
 146 molar volume.^{33, 34}

147 The dissipative force F^D and the random force F^R are expressed by:

$$148 \quad F_{ij}^D = -\gamma\omega^D(r_{ij})(\hat{r}_{ij} \cdot \bar{v}_{ij})\hat{r}_{ij} \quad (6)$$

$$149 \quad F_{ij}^R = \sigma\omega^R(r_{ij})\theta_{ij}\hat{r}_{ij} \quad (7)$$

150 where ω^D and ω^R are weight functions vanishing for $r > r_c$, $\bar{v}_{ij} = \bar{v}_j - \bar{v}_i$, γ is the friction
 151 coefficient, σ is the noise amplitude, and θ_{ij} is a randomly fluctuating variable with
 152 Gaussian statistics. The two weight functions can be taken simply as

$$153 \quad \omega^D(r) = [\omega^R(r)]^2 = \begin{cases} (1 - r/r_c)^2 & (r < r_c) \\ 0 & (r \geq r_c) \end{cases} \quad (8)$$

$$154 \quad \sigma^2 = 2\gamma k_B T \quad (9)$$

155 A simulated box size was fixed at $25 \times 25 \times 25 r_c^3$ with periodic boundary conditions.

156 With the reduced bead density ρ ($=r_c^3/V_m$) is 3, bead density of 3, the box contained
157 about 47,000 DPD beads, 10% of which was used for the polymer molecules. The coarse-
158 grained structure of POX triblock copolymer was drawn as Figure 1. The time step and
159 harmonic spring constant were taken as 0.05 and 4, respectively. The simulation took a total
160 of 2×10^5 DPD steps to guarantee the equilibration of the system. The equilibrium states were
161 confirmed through monitoring pressure, temperature, density and radius of gyration of
162 micelle. In Table 2, the repulsive parameters used in this DPD simulation are summarized.
163 According to Groot and Warren,¹⁹ $a_{ii} = 25$ was determined to obtain a compressibility of
164 liquid water and is broadly used for liquid systems in general. Three independent simulations
165 were performed for each system and the results were averaged.

166 To quantitatively analyze the simulated micellar structures, radial distribution
167 function (RDF) was utilized. The RDF, which is usually denoted by $g(r)$, is calculated by the
168 following equation:

$$169 \quad g_{COM-polymer}(r) = \left(\frac{n_{polymer}}{4\pi r^2 \Delta r} \right) / \left(\frac{N_{polymer}}{V} \right) \quad (10)$$

170 where $n_{polymer}$, V , and $N_{polymer}$ denote the number of particle found in a shell ($4\pi r^2 \Delta r$) apart
171 from the center of mass of micelle by the distance (r), the total volume of simulated system,
172 and the total number of particle in the simulated system, respectively.

173

174 3. RESULTS AND DISCUSSION

175 Total 5 systems were simulated to investigate how the reactant molecules were
176 distributed through the multicompartment micelle. The block sequence of $A_{50}B_2C_2$ was
177 employed: the block A, B and C represent PMOX, PBOX and PSCoX, respectively.

178 First, a bare micelle system was simulated without reactant molecules. From Figure 2a, it is
179 observed that the hydrophobic blocks (red color) form the micelle core by minimizing the

180 undesirable contact with solvent phase and other types of blocks, while the hydrophilic shell
181 is also formed to wrap the core from the external solvent phase. From the RDF of the
182 polymer blocks (Figure 2b), it is also observed that each domain has shell structure within the
183 micelle system: the core domain (block C, red color) is located from the center of the micelle
184 up to $5r_c$, while the most of block A (blue color) is distributed in the outermost region ranging
185 from $2r_c$ to $7r_c$. Clearly, the polymer block phases are significantly overlapped. However, it
186 should be noted that such internal structure can be better-defined by increasing block length
187 since the value of χN increases with increasing N and thereby the phase-separation will
188 develop more.

189 In the following sections, the distribution of reactant molecules in the micellar
190 structure is presented. In each case, total 450 molecules of reactant molecules were added to
191 the micelle system (equivalent to 1.1 mol %).

192

193 3.1. Reac-OPh and Reac-C4

194 In Figure 3a, due to the weak repulsive interaction between Reac-OPh molecules and
195 polymer blocks, numerous reactant molecules are associated in the hydrophilic domain (block
196 A). In addition, some amount of reactant molecules are located around the core domain.
197 According to the RDF shown in Figure 3b, it is confirmed that the reactant molecules are
198 well accommodated in the hydrophilic shell consisting of block A from $3r_c$ and $8r_c$. It seems
199 that there are a few reactant molecules in the hydrophobic core domain.

200 Figure 4a shows that Reac-C4 molecules are well dispersed in micelle, which is
201 comparable to Reac-OPh. Both cases demonstrated a strong evidence (Figure 4b) confirming
202 that the high solubility of reactant molecules enhances the molecular association of reactants
203 with the hydrophilic shell of micelle, and results in the high accessibility of reactant to the

204 reactive sites in the micelle core.

205 The important finding from these simulations with two reactants is that these
206 reactants have higher rate of HKR compared to other cases. From this, it is concluded that
207 this higher rate of HKR is correlated with the miscibility of the reactants with the micelle. We
208 think this is because the miscibility is a component of the permeation of reactants into the
209 reactive core of micelle.

210 **3.2. Reac-Ph and Reac-Cl**

211 In our previous studies,¹⁴ Reac-Ph and Reac-Cl were characterized to be less miscible
212 in the micelle structure compared to Reac-OPh and Reac-C4, which is well described in our
213 DPD simulations as illustrated in Figures 5 and 6. Figure 5a shows that Reac-Ph molecules
214 form a cluster on the micelle surface, instead of being incorporated into the micelle due to the
215 poor miscibility of Reac-Ph. Hence, the results observed from DPD simulations lead to the
216 conclusion that the slow HKR of Reac-Ph is straightforwardly attributed to the poor
217 miscibility between Reac-Ph and micelle.

218 Another reactant (Reac-Cl) with the slow rate also exhibits a poor incorporation into
219 the micelle as similarly observed in the case of Reac-Ph. Unlike the system with Reac-Ph,
220 Reac-Cl molecules are spread over the surface of the micelle and enter the hydrophilic shell
221 to some extent, which is consistent with the observation in Figure 6b. We think that this
222 difference is well explained by the repulsive interaction parameters reported in Table 1. With
223 respect to PMOX, PBOX and PSCoX, the repulsive interaction parameters (a_{ij}) of Reac-Ph
224 have greater values than those of Reac-Cl, which means that Reac-Ph undergoes more
225 exclusion from the micelle. Besides, the larger value of a_{ij} of Reac-Cl against water phase
226 plays a role in driving the Reac-Cl molecules into the hydrophilic shell more.

227 **3.3. Comparison with Previous χ_{FH} Parameters**

228 In our previous study,¹⁴ The χ_{FH} parameters were calculated as a function of
229 compositions. Moreover, the energy of mixing was independently calculated from the mixed
230 systems. In contrast, the χ_{FH} parameters used for DPD simulations are calculated using the
231 δ parameters without considering the concentration (or composition) as expressed by
232 Equation (5). For this reason, it seems to be necessary to compare one set of parameters to
233 another in order to identify any possible deficiency in the current scheme of χ_{FH} parameter
234 calculation and its solutions to improve the quality of parameters.

235 Figure 7 shows the comparison of χ_{FH} parameters for variety of reactant with respect
236 to a polymer (Figure 7a) and variety of polymer with respect to a reactant (Figure 7b). First, it
237 is found from the most cases that the values of χ_{FH} parameters calculated from the δ
238 parameters for DPD simulations are smaller than those calculated from our previous MD
239 simulation study. Although it seems to be obvious because the different χ_{FH} parameters can be
240 resulted from the different theories, it is noted that the χ_{FH} parameters calculated from the MD
241 simulations with the composition of 70 wt% reactant shows similar trend to those calculated
242 from the δ parameters. We think that this is because the δ parameter is calculated from
243 the condensed phase, and the composition of 70 wt% provides a similar condition of the
244 condensed phase as used in the calculation of δ parameters. Considering that the phase
245 separation or segregation are determined by relative miscibility or immiscibility among
246 components, it is anticipated that that the phase segregation described using χ_{FH} parameters
247 with the composition of 70 wt% reactant would be in agreement with the phase segregation
248 using δ -based χ_{FH} parameters.

249 Another point in Figure 7a is that the χ parameters for Reac-OPh and Reac-C4 are
250 smaller than those for Reac-Cl and Reac-Ph with respect to PMOX, which confirms that our
251 understanding based on the simulated χ parameters has a good predictability for HKR of

252 epoxides. This means that Reac-OPh and Reac-C4 have better miscibility with the micelle
253 corona than Reac-Cl and Reac-Ph, which is in a good agreement with the observation of the
254 previous publication.¹⁴ In other words, Reac-OPh and Reac-C4 are expected to be associated
255 more with the micelle corona compared to Reac-Cl and Reac-Ph.

256 Figure 7b presents the change of χ parameter of Reac-OPh with polymer blocks such
257 as PMOX, PBOX and PSCoX, which provides an evaluation of χ parameter as Reac-OPh
258 diffuses into the micelle from corona to core. First, at lower concentration conditions, namely,
259 15 wt% and 45 wt%, the value of χ parameter with the core is smaller, meaning that Reac-
260 OPh is miscible with the core (PSCoX, the reactive site of HKR) more than with corona
261 (PMOX) and mid-shell (PBOX). On the contrary, the χ parameter monotonously increases at
262 higher concentration condition, meaning that diffusion of Reac-OPh towards the core of
263 micelle becomes more difficult, which is also observed that the solubility-based χ parameter
264 in DPD simulation. Here, please note that HKR occurs at the core of micelle, indicating that
265 Reac-OPh will be consumed at the core. Then the concentration at the core will be reduced,
266 which will facilitate new provision of Reac-OPh into the core.

267 By considering this χ parameter as well as the distribution through the micelle, it is
268 conclusively clear that the HKR has strong correlation with the miscibility (or solubility) of
269 reactant with micellar nanoreactor.

270

271 4. SUMMARY

272 DPD simulation method was employed to simulate the multicompartment micelle
273 consisting of 71 POX-based triblock copolymers ($A_{50}B_2C_2$). The DPD parameters were
274 determined according to the Flory-Huggins interaction parameter (χ_{FH}) calculated from the
275 Hildebrand solubility parameters (δ). Both the coarse-grained molecular models and the

276 RDF data from DPD simulations confirm that the micelle has the feature of the
277 multicompartment.

278 Next, the incorporation of reactant molecules into the multicompartment micelle was
279 investigated. The simulations showed that Reac-C4 and Reac-OPh are well associated with
280 the micelle, especially in the hydrophilic shell whereas Reac-Ph and Reac-Cl are not mixed
281 with the hydrophilic shell. These findings are in a good agreement with the previous
282 experiment⁴ and simulation study,¹⁴ reporting that the miscibility (solubility) of reactant with
283 the micelle has strong correlation with the rate of HKR.

284 Using DPD method, the entire micelles with detailed internal multicompartment
285 micelles feature were efficiently simulated in the presence of water phase, and the
286 distributions of reactants through this multicompartment micelle were quantitatively
287 characterized. By combining accurate method evaluating χ_{FH} parameters for molecular
288 interactions in micelle system, this DPD simulation protocol can be applied for selecting
289 promising candidates for higher rate of HKR.

290

291 5. ACKNOWLEDGMENTS

292 This research was supported by the Department of Energy (DE-FG02-03ER15459). We also
293 acknowledge that this research used resources of the Keeneland Computing Facility at the
294 Georgia Institute of Technology, supported by the National Science Foundation under
295 Contract OCI-0910735.

296

297 6. REFERENCES

- 298 1. R. Chandrawati, M. P. Van Koeverden, H. Lomas and F. Caruso, *Journal of Physical*
299 *Chemistry Letters*, 2011, **2**, 2639-2649.
300 2. V. Balasubramanian, O. Onaca, M. Ezhevskaya, S. Van Doorslaer, B. Sivasankaran and
301 C. G. Palivan, *Soft Matter*, 2011, **7**, 5595-5603.

- 302 3. P. Cotanda, A. Lu, J. P. Patterson, N. Petzetakis and R. K. O'Reilly, *Macromolecules*,
303 2012, **45**, 2377-2384.
- 304 4. Y. Liu, Y. Wang, Y. Wang, J. Lu, V. Piñón and M. Weck, *Journal of the American*
305 *Chemical Society*, 2011, **133**, 14260-14263.
- 306 5. A. Lu, P. Cotanda, J. P. Patterson, D. A. Longbottom and R. K. O'Reilly, *Chemical*
307 *Communications*, 2012, **48**, 9699-9701.
- 308 6. M. J. Monteiro, *Macromolecules*, 2010, **43**, 1159-1168.
- 309 7. O. Onaca, D. W. Hughes, V. Balasubramanian, M. Grzelakowski, W. Meier and C. G.
310 Palivan, *Macromolecular Bioscience*, 2010, **10**, 531-538.
- 311 8. K. Renggli, P. Baumann, K. Langowska, O. Onaca, N. Bruns and W. Meier, *Advanced*
312 *Functional Materials*, 2011, **21**, 1241-1259.
- 313 9. A. Lu and R. K. O'Reilly, *Current Opinion in Biotechnology*, 2013, **24**, 639-645.
- 314 10. R. K. O'Reilly, C. J. Hawker and K. L. Wooley, *Chemical Society Reviews*, 2006, **35**,
315 1068-1083.
- 316 11. Y. Liu, V. Piñón and M. Weck, *Polymer Chemistry*, 2011, **2**, 1964-1975.
- 317 12. P. Tanner, O. Onaca, V. Balasubramanian, W. Meier and C. G. Palivan, *Chemistry- A*
318 *European Journal*, 2011, **17**, 4552-4560.
- 319 13. A. Lu, T. P. Smart, T. H. Epps, D. A. Longbottom and R. K. O'Reilly, *Macromolecules*,
320 2011, **44**, 7233-7241.
- 321 14. B. J. Chun, J. Lu, M. Weck and S. S. Jang, *Physical Chemistry Chemical Physics*, 2015,
322 **17**, 29161-29170.
- 323 15. P. J. Hoogerbrugge and J. M. V. A. Koelman, *Europhysics Letters*, 1992, **19**, 155.
- 324 16. J. Koelman and P. J. Hoogerbrugge, *Europhysics Letters*, 1993, **21**, 363-368.
- 325 17. S. G. Schulz, H. Kuhn, G. Schmid, C. Mund and J. Venzmer, *Colloid and Polymer*
326 *Science*, 2004, **283**, 284-290.
- 327 18. V. Symeonidis, G. E. Karniadakis and B. Caswell, *Physical Review Letters*, 2005, **95**.
- 328 19. R. D. Groot and P. B. Warren, *Journal of Chemical Physics*, 1997, **107**, 4423-4435.
- 329 20. R. D. Groot, *Journal of Chemical Physics*, 2003, **118**, 11265-11277.
- 330 21. P. J. Hoogerbrugge and J. Koelman, *Europhysics Letters*, 1992, **19**, 155-160.
- 331 22. J. H. Huang, Y. M. Wang and M. Laradji, *Macromolecules*, 2006, **39**, 5546-5554.
- 332 23. H. J. Qian, Z. Y. Lu, L. J. Chen, Z. S. Li and C. C. Sun, *Macromolecules*, 2005, **38**,
333 1395-1401.
- 334 24. D. H. Liu and C. L. Zhong, *Macromolecular Rapid Communications*, 2005, **26**, 1960-
335 1964.
- 336 25. D. H. Liu and C. L. Zhong, *Macromolecular Rapid Communications*, 2006, **27**, 458-462.
- 337 26. Y. Xu, J. Feng, H. Liu and Y. Hu, *Molecular Simulation*, 2006, **32**, 375-383.
- 338 27. C. L. Zhong and D. H. Liu, *Macromolecular Theory and Simulations*, 2007, **16**, 141-157.
- 339 28. S. Yamamoto, Y. Maruyama and S.-a. Hyodo, *Journal of Chemical Physics*, 2002, **116**,
340 5842-5849.
- 341 29. Y. Tang, S. Y. Liu, S. P. Armes and N. C. Billingham, *Biomacromolecules*, 2003, **4**,
342 1636-1645.
- 343 30. R. S. Underhill and G. Liu, *Chemistry of Materials*, 2000, **12**, 3633-3641.
- 344 31. X. Li, I. V. Pivkin, H. Liang and G. E. Karniadakis, *Macromolecules*, 2009, **42**, 3195-
345 3200.
- 346 32. J.-F. Gohy, N. Willet, S. Varshney, J.-X. Zhang and R. Jérôme, *Angewandte Chemie*
347 *International Edition*, 2001, **40**, 3214-3216.
- 348 33. M. Belmares, M. Blanco, W. A. Goddard, R. B. Ross, G. Caldwell, S. H. Chou, J. Pham,
349 P. M. Olofson and C. Thomas, *J. Comput. Chem.*, 2004, **25**, 1814-1826.

350 34. A. F. M. Barton, *Chem. Rev.*, 1975, **75**, 731-753.

351

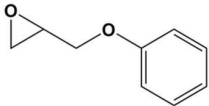
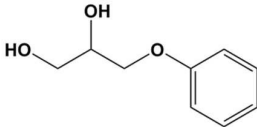
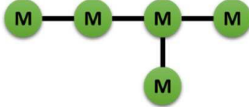
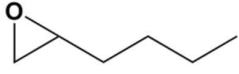
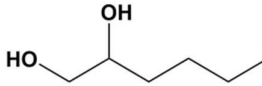
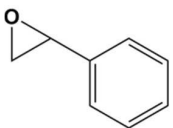
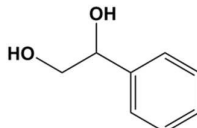
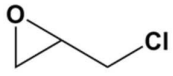
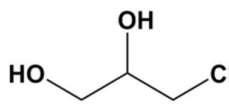
352

353

354

355
356
357
358
359
360
361
362

Table 1. Chemical structures of reactant and product molecules and their coarse-grained model in DPD simulation. Water molecule was also coarse grained by single bead in this simulation scheme

Entry	Atomistic Chemical Structure	Coarse-Grained Model	
1	 Phenyl glycidyle ether (Reac-OPh)	 Phenol glycerol ether (Pro-OPh)	
2	 Epoxyhexane (Reac-C4)	 Hexane diol (Pro-C4)	
3	 Styrene oxide (Reac-Ph)	 Phenylethane diol (Pro-Ph)	
4	 Epichlorohydrine (Reac-Cl)	 Chloropropane diol (Pro-Cl)	

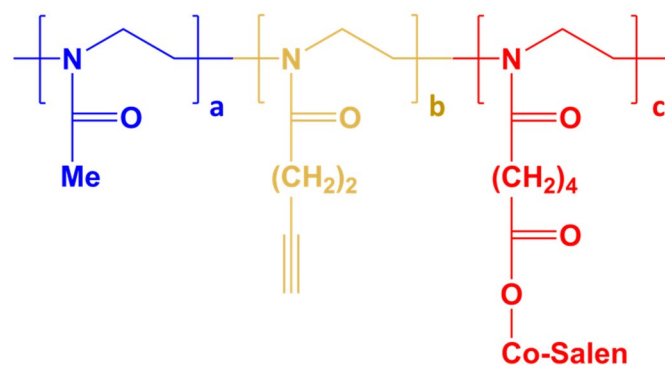
363
364
365

366
367
368
369
370
371
372
373
374

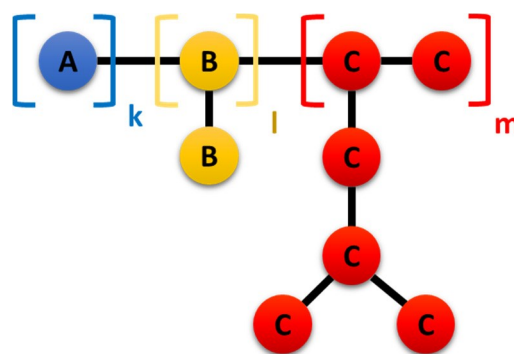
Table 2. Repulsive interaction parameters (a_{ij} in Equation (4)) among the components in DPD simulation system. A, B, C, and W denote PMOX, PBOX, PSCoX and water solvent, respectively. Since each simulation includes only one type of reactant or product molecules with the polymer micelle, there is no parameter among reactant and product molecules

	A (PMOX)	B (PBOX)	C (PSCoX)	W (Water)
A	25.00	-	-	-
B	25.01	25.00	-	-
C	26.60	26.34	25.00	-
W	83.57	85.23	104.56	25.00
Reac-OPh	25.84	26.17	32.93	136.35
Reac-C4	25.00	25.04	28.70	155.98
Reac-Ph	36.38	37.50	52.79	90.56
Reac-Cl	30.46	31.24	42.93	108.43

375
376
377
378



(a)



(b)

Figure 1. Chemical structures of POX derivatives and their coarse-grained models in DPD simulation: (a) Blue, yellow, and red colored structures represent poly(2-methyl-2-oxazoline) (PMOX), poly(2-(3-butynyl)-2-oxazoline) (PBOX), and poly(methyl-3-oxazol-2-yl) pentanoate with Co(III)-salen (PSCoX), respectively; (b) Likewise, blue, yellow, and red colored beads denote the coarse-grained PMOX, PBOX, and PSCoX, respectively.

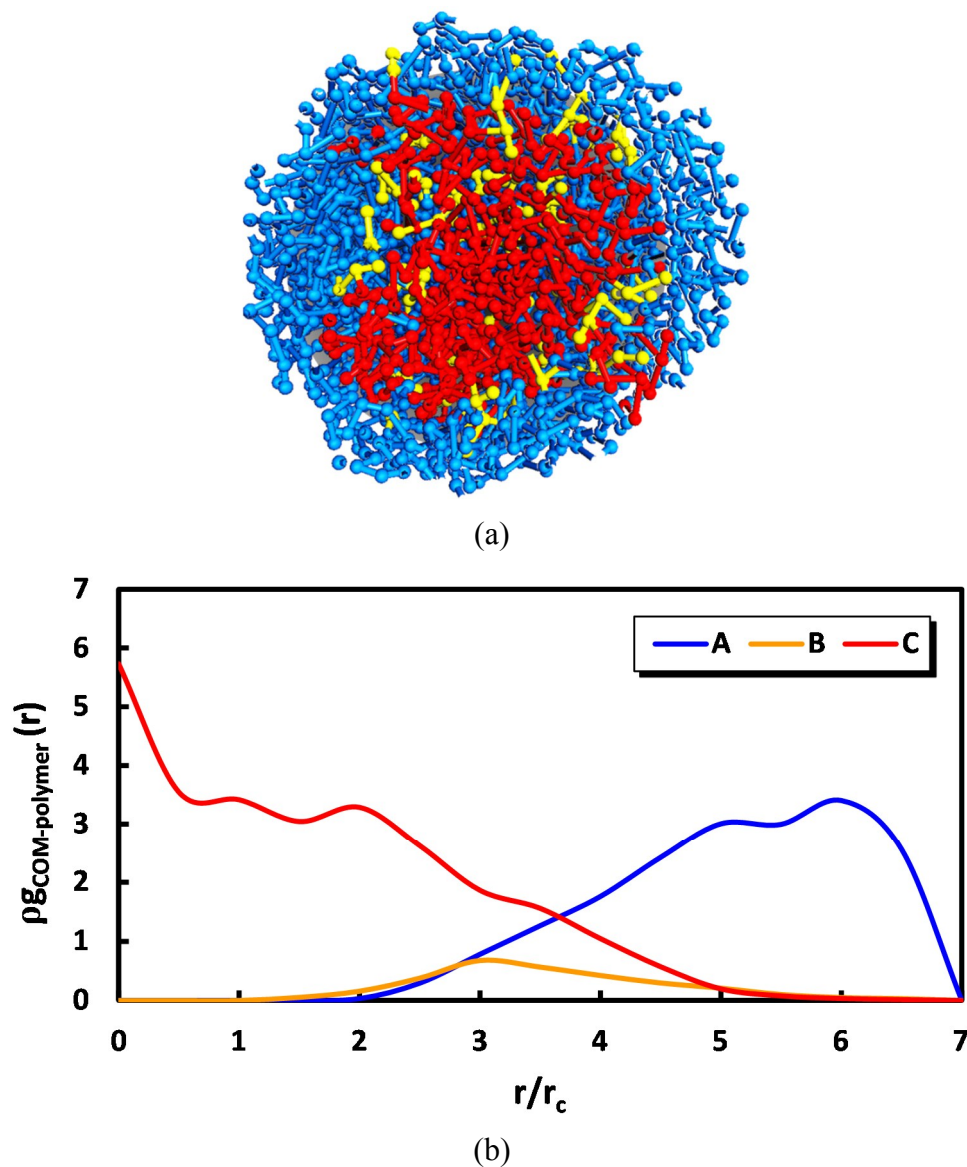


Figure 2. DPD simulation of bare micelle: (a) the cross-sectional view of micelle structure; (b) the RDF of three components from the center of the micelle. Blue, yellow, and red colored regions indicate block A, B, and C (the coarse-grained PMOX, PBOX, and PSCoX blocks), respectively

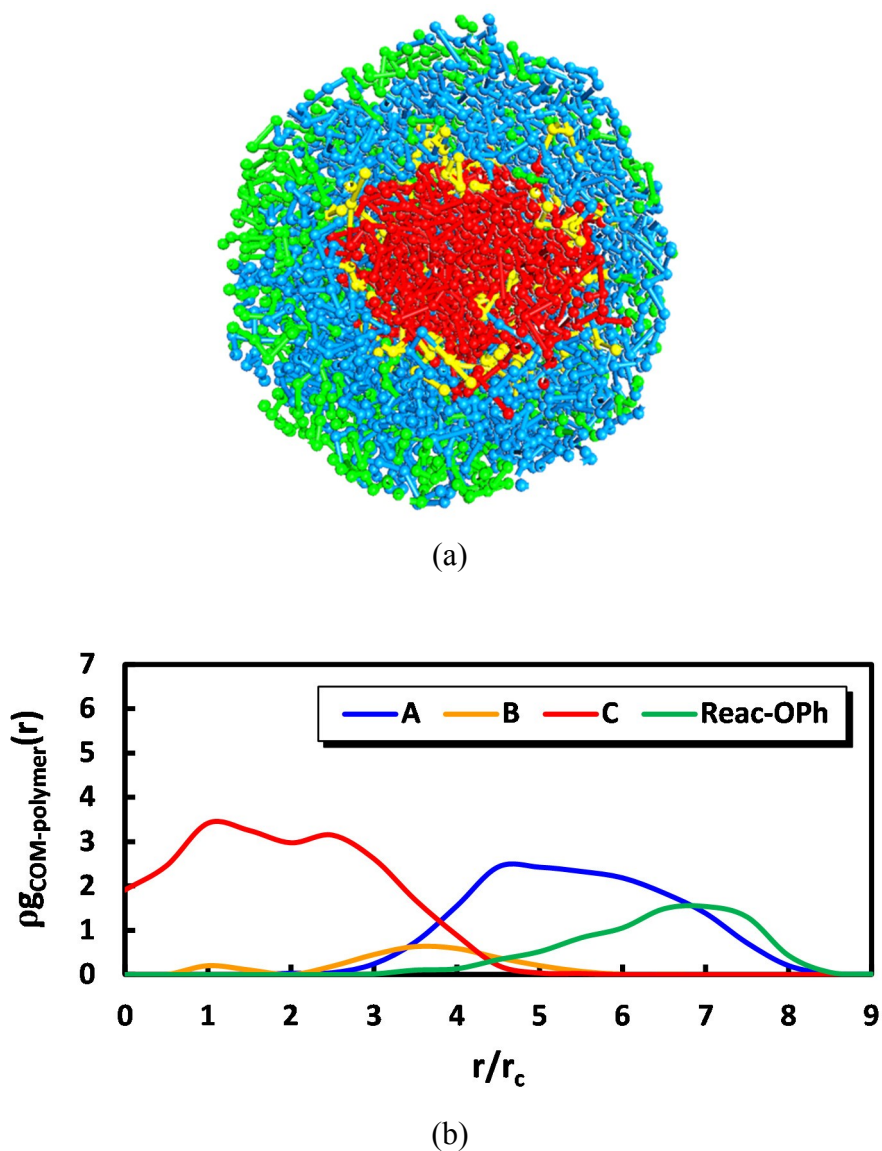


Figure 3. DPD simulation of micelle with Reac-OPh: (a) the cross-sectional view of micelle structure; (b) the RDF of four components from the center of the micelle. Blue, yellow, red, and green colored regions indicate bead A, B, C (the coarse-grained PMOX, PBOX, and PSCoX blocks), and Reac-OPh, respectively.

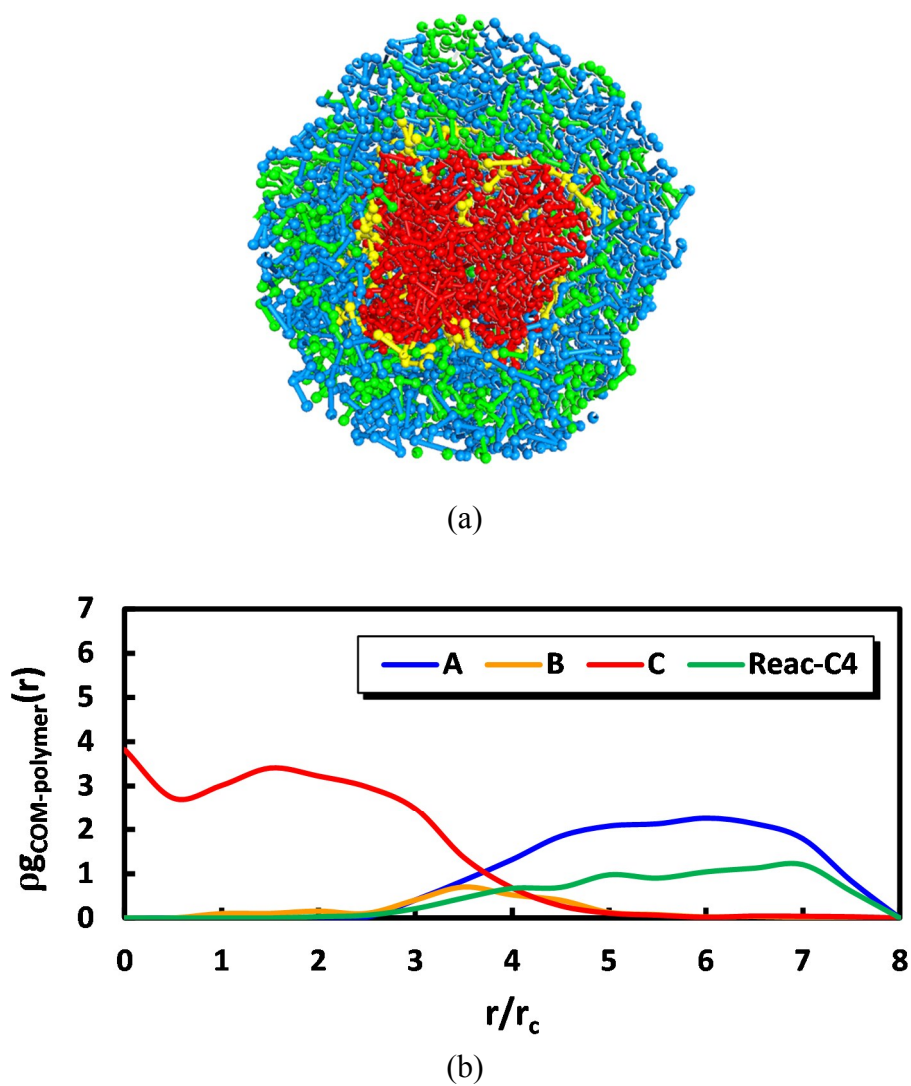


Figure 4. DPD simulation of micelle with Reac-C4: (a) the cross-sectional view of micelle structure; (b) the RDF of four components from the center of the micelle. Blue, yellow, red, and green colored regions bead A, B, C (the coarse-grained PMOX, PBOX, and PSCoX blocks), and Reac-C4, respectively.

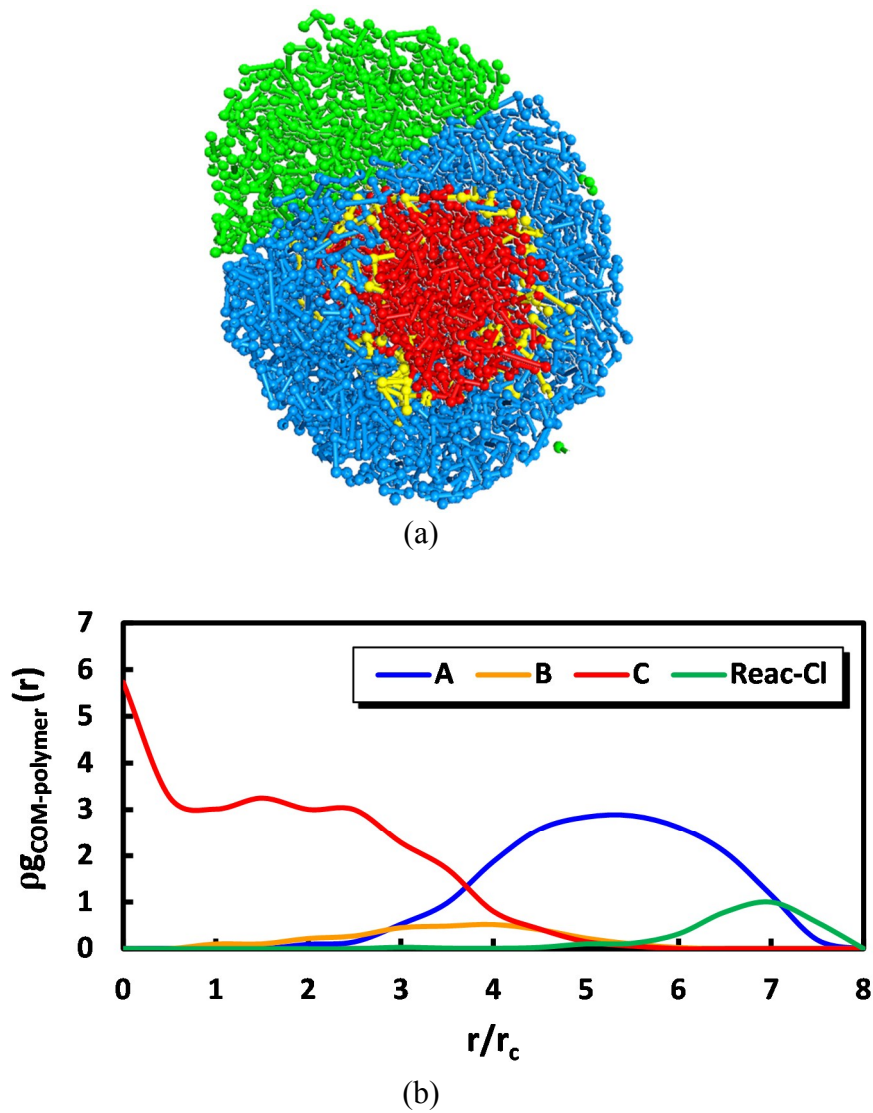


Figure 5. DPD simulation with Reac-Ph: (a) the cross-sectional view of micelle structure; (b) the RDF of four components from the center of the micelle. Blue, yellow, red, and green colored regions indicate bead A, B, C (the coarse-grained PMOX, PBOX, and PSCoX blocks), and Reac-Ph, respectively.

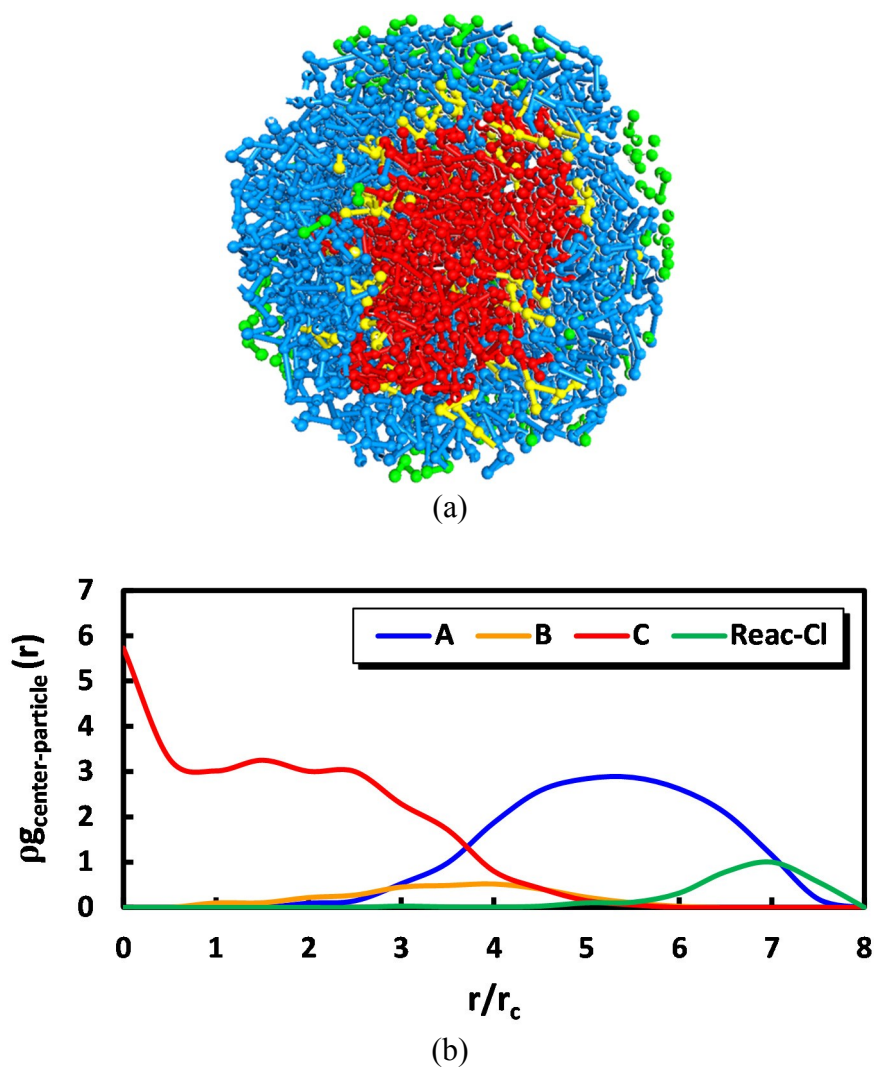
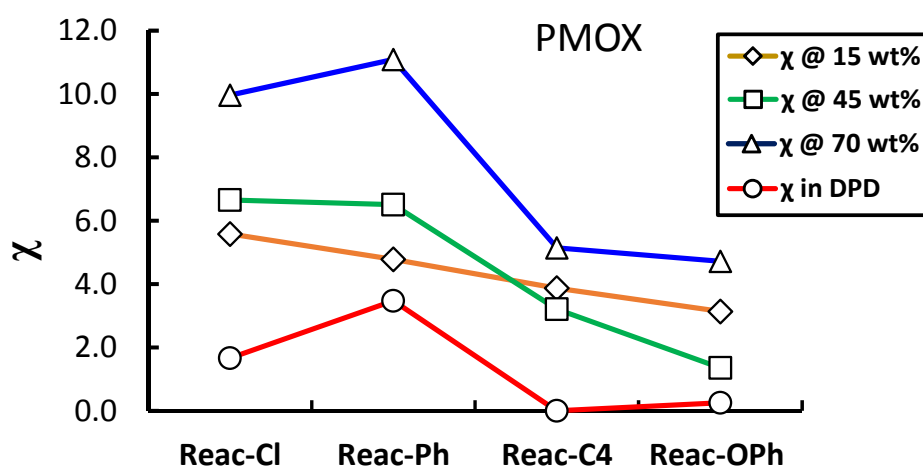
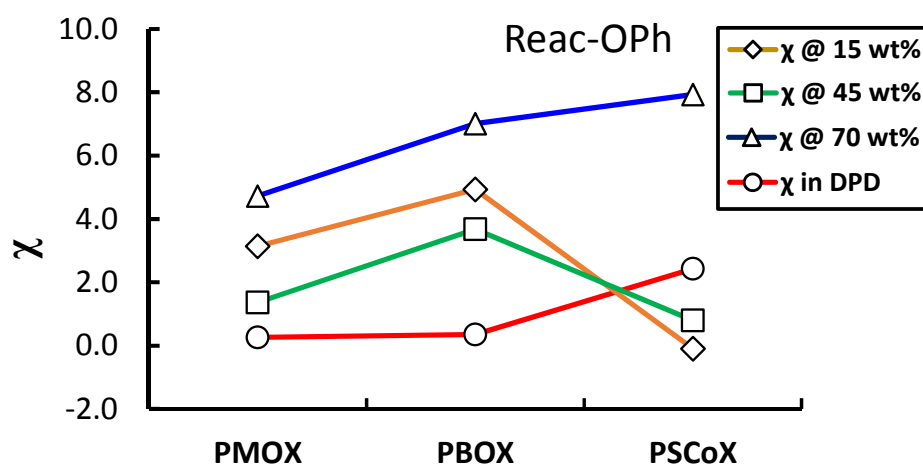


Figure 6. DPD simulation with Reac-Cl: (a) the cross-sectional view of micelle structure; (b) the RDF of four components from the center of the micelle. Blue, yellow, red, and green colored regions indicate bead A, B, C (the coarse-grained PMOX, PBOX, and PSCoX blocks), and Reac-Cl, respectively.



(a)

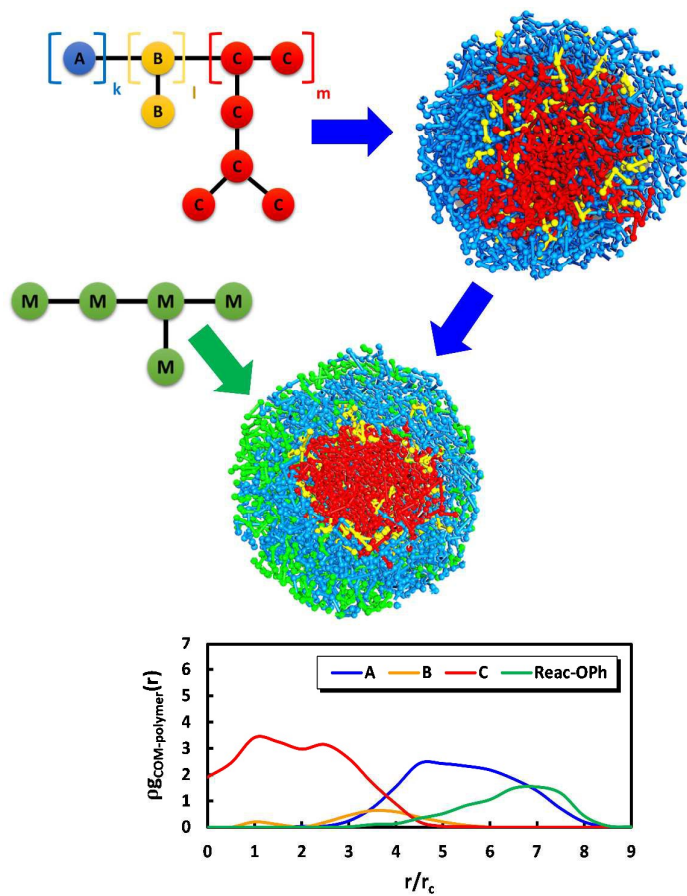


(b)

Figure 7. Comparison of χ_{FH} parameters: (a) for various reactants with respect to a common polymeric block (PMOX); (b) for various polymeric blocks with respect to a common reactant (React-OPh). Only “ χ in DPD” is obtained from coarse-grained models while all others are from full-atomistic models.

1
2
3
4
5
6
7
8

GRAPHIC ABSTRACT

9
10
11
12
13